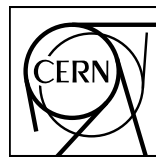


EUROPEAN ORGANIZATION FOR NUCLEAR RESEARCH



CERN-EP-2023-248
03 November 2023

Photoproduction of K^+K^- pairs in ultra-peripheral collisions

ALICE Collaboration*

Abstract

K^+K^- pairs may be produced in photonuclear collisions, either from the decays of photoproduced $\phi(1020)$ mesons, or directly as non-resonant K^+K^- pairs. Measurements of K^+K^- photoproduction probe the couplings between the $\phi(1020)$ and charged kaons with photons and nuclear targets. The kaon–proton scattering occurs at energies far above those available elsewhere. We present the first measurement of coherent photoproduction of K^+K^- pairs on lead ions in ultra-peripheral collisions using the ALICE detector, including the first investigation of direct K^+K^- production. There is significant K^+K^- production at low transverse momentum, consistent with coherent photoproduction on lead targets. In the mass range $1.1 < M_{KK} < 1.4 \text{ GeV}/c^2$ above the $\phi(1020)$ resonance, for rapidity $|y_{KK}| < 0.8$ and $p_{T,KK} < 0.1 \text{ GeV}/c$, the measured coherent photoproduction cross section is $d\sigma/dy = 3.37 \pm 0.61 \text{ (stat.)} \pm 0.15 \text{ (syst.) mb}$. The center-of-mass energy per nucleon of the photon–nucleus (Pb) system $W_{\gamma\text{Pb},n}$ ranges from 33 to 188 GeV, far higher than previous measurements on heavy-nucleus targets. The cross section is larger than expected for $\phi(1020)$ photoproduction alone. The mass spectrum is fit to a cocktail consisting of $\phi(1020)$ decays, direct K^+K^- photoproduction, and interference between the two. The confidence regions for the amplitude and relative phase angle for direct K^+K^- photoproduction are presented.

Introduction. High-energy photoproduction is an important technique for studying hadronic interactions. Ultra-peripheral collisions (UPCs) of relativistic ions are a tool for studying photonuclear interactions at energies far higher than those available elsewhere [1–4]. The electromagnetic field of one nucleus forms an intense virtual-photon beam that can interact with nuclei from the opposing beam. UPC interactions occur when the impact parameter (b) between the two nuclei is large enough, e.g. b is greater than the sum of the nuclear radii, so that no obscuring hadron–hadron interactions occur.

A photon can fluctuate into a quark-antiquark pair (dipole) that scatters elastically from a target nucleus, emerging as a real vector meson [5]. The elastic scattering is mediated by the Pomeron, which is a colorless object and to lowest order, composed of two gluons. The exchange involves the quantum numbers of the vacuum, so following the Vector Meson Dominance (VMD) model, the outgoing meson has the same quantum numbers $J^{PC} = 1^{--}$ as the incident photon [6]. Alternatively, the photon can fluctuate directly into a virtual meson pair, like $\pi^+\pi^-$ or K⁺K⁻. One of the mesons can then scatter elastically from the target, making the pair real. For midrapidity kaons in ALICE, the kaon–proton center of mass energy is 50 GeV, far higher than can be studied elsewhere. Exclusive K⁺K⁻ production can also occur via two-photon [7] or in double-Pomeron interactions [8], but this is the first observation in the photon–Pomeron channel.

Since the channels are indistinguishable, meson pairs from the decay of vector mesons ($\rho^0 \rightarrow \pi^+\pi^-$ or $\phi(1020) \rightarrow K^+K^-$) can interfere with the directly produced pairs. The production amplitude has two terms: the resonance is described using a Breit-Wigner distribution expressed in the Jackson form, with amplitude A_ϕ , and there is, in addition, a continuum component with amplitude B_{KK} [9–11], giving

$$\frac{d\sigma}{dM_{KK}} = \left| A_\phi \frac{\sqrt{M_{KK}M_\phi\Gamma_\phi}}{M_{KK}^2 - M_\phi^2 + iM_\phi\Gamma_\phi} + B_{KK} \right|^2, \quad (1)$$

where $M_\phi = 1019.416 \pm 0.016$ MeV/c² [12] and Γ_ϕ are the $\phi(1020)$ mass and mass-dependent width, respectively, with

$$\Gamma_\phi = \Gamma_0 \frac{M_\phi}{M_{KK}} \left(\frac{M_{KK}^2 - 4M_K^2}{M_\phi^2 - 4M_K^2} \right)^{3/2}. \quad (2)$$

Here, $\Gamma_0 = 4.249 \pm 0.013$ MeV/c² is the native $\phi(1020)$ width, and $M_K = 493.677 \pm 0.016$ MeV/c² is the kaon mass [12]. Both A_ϕ and B_{KK} are complex, but only their relative phase matters. By taking A_ϕ to be real, the relative phase is encoded in B_{KK} . Far above the $\phi(1020)$ resonance (many Γ_0), the mass-dependent width rises, and the cross section declines smoothly. One difference between the K⁺K⁻ and $\pi^+\pi^-$ systems is that the branching ratio $\phi(1020) \rightarrow K^+K^-$ is only 49.1% [12], while the ρ^0 almost always decays to $\pi^+\pi^-$. This branching ratio is included in A_ϕ . Ryskin and Shabelski considered the direct dikaon contribution to the total dikaon cross section, and concluded that it should be small and with a relative phase angle near zero [13]. A later calculation predicted that the dikaon system should behave similarly to the dipions, with a small correction to the width to account for three-body $\phi(1020)$ decays [11].

The transverse momentum p_T of the meson depends on the production mechanism, so it is important in selecting coherent photoproduction events, where a dipole or virtual meson pair scatters from the target nucleus. The meson p_T is the vector sum of the photon p_T and the Pomeron p_T , which usually dominates [14]. For coherent production, its scale is controlled by the form factor of the target nucleus. Destructive interference between the amplitudes for production on the two nuclei can reduce the cross section at low p_T , especially near midrapidity [14, 15]. In incoherent production, when a dipole or virtual meson pair scatters from a single nucleon, the typical p_T is larger, around a few hundred MeV/c. Although Pomeron–Pomeron interactions can also produce exclusive K⁺K⁻ pairs [8], because of the short range of the strong force, these reactions cannot be coherent over the entire nuclei, and, so, will not produce a peak at low p_T and do not contribute to the current coherent measurement.

Previously, $\phi(1020)$ photoproduction has been studied at fixed-target experiments [6, 16] and the HERA ep collider [17–19]. However, the direct K⁺K⁻ contribution has not yet been observed. The H1 Collaboration searched for skewing in the ϕ Breit-Wigner peak due to direct K⁺K⁻ production (in electro-production), but found no evidence for it [19]. In contrast, the ρ^0 + direct $\pi^+\pi^-$ state has been studied in both UPCs [20–25] and, at lower energy, at fixed-target experiments [6]. The $\pi^+\pi^-$ mass spectra are well fit by the sum of amplitudes for ρ^0 and direct $\pi^+\pi^-$, with a high-statistics fit exhibiting additional interference from $\omega \rightarrow \pi^+\pi^-$ [22, 26]. Higher-mass $\pi^+\pi^-$ states have also been seen [23, 27, 28].

This Letter reports on exclusive photoproduction of the K⁺K⁻ final state, from the decay of the $\phi(1020)$ and direct production. The data cover the mass region $1.1 < M_{KK} < 1.4$ GeV/c². This is significantly above the $\phi(1020)$ peak, with the lower mass limit at about $M_\phi + 18\Gamma_0$.

The cross sections are measured at the center-of-mass energy per nucleon of the photon–nucleus (Pb) system $W_{\gamma\text{Pb},n}$, where $W_{\gamma\text{Pb},n}$ varies from 33 to 188 GeV, depending on M_{KK} and rapidity. This range of energies is more than an order of magnitude higher than previous studies using heavy-nucleus targets [6, 16].

Detector and data. The results presented in this Letter are based on the data collected in 2015 by the ALICE experiment [29, 30], with Pb–Pb collisions at a center-of-mass energy per nucleon pair $\sqrt{s_{\text{NN}}} = 5.02$ TeV. A dedicated trigger was used to select candidate UPC events [23], rejecting any activity within the time windows for nominal beam–beam interactions, using the scintillator detectors V0 [31] and AD [32, 33] located at large positive and negative pseudorapidity. In addition, the trigger required that the Silicon Pixel Detector (SPD), the two innermost layers of the inner tracking system (ITS) [34], measured at least two short track segments with a large opening angle in azimuth.

The time projection chamber (TPC) covering the pseudorapidity acceptance of $|\eta| < 0.9$ was used for charged particle tracking and vertexing together with the ITS as well as for particle identification based on the specific ionization energy loss, dE/dx [35].

Analysis Procedure. The analysis selected events with exactly two good tracks. The tracks were required to have at least 50 hits (clusters) in the TPC, at least one hit in each of the two layers of the SPD, and to have the distance-of-closest approach to the event vertex of less than $0.0182 + 0.035/p_T^{1.01}$ cm in the transverse plane and less than 2 cm along the beam direction. The two selected tracks having opposite charge are reconstructed as K⁺K⁻ pair candidates under the kaon mass hypothesis. As there are no same-charge pairs passing the particle identification criteria, the contribution of uncorrelated background could be ignored in this analysis.

Kaons are identified based on the dE/dx measurement in the TPC. The selection criteria are applied to the variable n_{σ_i} , the deviation of the measured signal from the expected signal in units of the dE/dx measurement uncertainty for each particle hypothesis i . Since the ratio of signal K⁺K⁻ pairs to background $\pi^+\pi^-$ pairs is less than 0.1%, stringent particle identification criteria are introduced. First, the tracks in each pair are required to satisfy $|n_{\sigma_K}| < 3$. In addition, the tracks which are compatible within $2n_{\sigma_{\pi,\mu,e}}$ are excluded to reject $\pi^+\pi^-$ pairs as well as dilepton pairs from the $\gamma\gamma \rightarrow l^+l^-$ process.

The contamination of the K⁺K⁻ pair candidates by the misidentified particles is estimated from the two-dimensional n_{σ_K} distribution of the two tracks in each pair. While the signal K⁺K⁻ pairs have a two-dimensional Gaussian-like distribution centered at (0,0), background pairs are clustered at non-zero values. For $1.1 < M_{KK} < 1.4$ GeV/c², the contamination is negligible as the signal and background distributions are well separated from each other. At higher masses, the expected difference in dE/dx between kaons and lighter particles decreases, so they become indistinguishable in some n_{σ_K} regions. Therefore, the invariant mass range above 1.4 GeV/c² is not used in the analysis. For pairs with $M_{KK} < 1.1$ GeV/c², the kaons lose energy rapidly and do not reach the sensitive region of the ALICE detector.

Measurement of the cross section. The invariant mass differential cross section of exclusive K⁺K⁻

photoproduction is obtained by correcting the number of K⁺K⁻ candidates (N_{KK}) found in the rapidity interval of $|y_{\text{KK}}| < 0.8$ and in the $p_{\text{T},\text{KK}}$ interval of $p_{\text{T},\text{KK}} < 0.1 \text{ GeV}/c$ by acceptance and efficiency ($\mathcal{A} \times \epsilon$),

$$\frac{d^2\sigma}{dM_{\text{KK}}dy_{\text{KK}}} = \frac{N_{\text{KK}} \times f_{\text{pileup}}}{(\mathcal{A} \times \epsilon) \times \mathcal{L} \times \Delta M_{\text{KK}} \times \Delta y_{\text{KK}}}. \quad (3)$$

The $\mathcal{A} \times \epsilon$ is computed using a dedicated Monte Carlo simulation with STARlight [36] for the K⁺K⁻ pairs from direct production and $\phi(1020)$ decays.

The generated K⁺K⁻ pairs are transported through the detector setup using a GEANT 3 model [37] to simulate a realistic detector response. The corresponding integrated luminosity (\mathcal{L}) for the data sample is $0.406 \mu\text{b}^{-1}$ with a relative systematic uncertainty of 2.6% [38]. Some events are lost due to pileup, when another interaction creates a signal in one of the veto detectors. The pileup events mainly come from two-photon production of e⁺e⁻ pairs, and their effect is taken into account with an additional correction factor, $f_{\text{pileup}} = 11.1 \pm 3.8\%$ [23]. Similarly, the p_{T}^2 -differential cross section of exclusive K⁺K⁻ photoproduction in $1.1 < M_{\text{KK}} < 1.4 \text{ GeV}/c^2$ is measured,

$$\frac{d^2\sigma}{dp_{\text{T},\text{KK}}^2 dy_{\text{KK}}} = \frac{N_{\text{KK}} \times f_{\text{pileup}}}{(\mathcal{A} \times \epsilon) \times \mathcal{L} \times \Delta p_{\text{T},\text{KK}}^2 \times \Delta y_{\text{KK}}}. \quad (4)$$

Systematic uncertainties. The systematic uncertainties of the measured cross section are estimated for the track selection criteria (1.5%) and the track matching between ITS and TPC (4%) as well as for the acceptance and efficiency (1%), without dependence on $p_{\text{T},\text{KK}}$, y_{KK} , and M_{KK} [23]. Uncertainties of 1% and 3.8% are included for the trigger efficiency and for the pileup correction, respectively [23]. The uncertainty of the luminosity (2.6%) results from the uncertainty of the reference luminosity in the cross section of 2.5% [38] and an additional 0.4% uncertainty on the live-time of readout detectors used for the trigger.

The systematic uncertainty of the kaon identification is estimated as a function of $p_{\text{T},\text{KK}}$ and M_{KK} to account for the track momentum dependence in the kaon identification performance. The expected signal of TPC dE/dx for each particle hypothesis is varied in the MC simulations by the maximum difference of the signal in data and MC simulations. Then, n_{σ_i} and the corresponding kaon identification efficiency are recalculated. The resulting uncertainty is negligible for $1.1 < M_{\text{KK}} < 1.2 \text{ GeV}/c^2$ and amounts to 3.9% and 6.5% for $1.2 < M_{\text{KK}} < 1.3 \text{ GeV}/c^2$ and $1.3 < M_{\text{KK}} < 1.4 \text{ GeV}/c^2$, respectively. The systematic uncertainty increases slowly as a function of $p_{\text{T},\text{KK}}$, from 3.4% for $p_{\text{T},\text{KK}} < 0.025 \text{ GeV}/c$ to 4.9% for $0.1 < p_{\text{T},\text{KK}} < 0.2 \text{ GeV}/c$. Over most of the kinematic range, this is the largest single systematic uncertainty.

Results. Figure 1 shows the p_{T}^2 spectrum of the selected K⁺K⁻ events. Most of the cross section is concentrated below $p_{\text{T},\text{KK}}^2 < 0.01 (\text{GeV}/c)^2$, consistent with coherent photoproduction. Some events are seen at higher values of $p_{\text{T},\text{KK}}^2$; these may be from incoherent production. The coherent data are well described with an exponential shape $d^2\sigma/dydp_{\text{T}}^2 = a \exp(-bp_{\text{T}}^2)$, where the slope parameter b is fixed to that measured for coherent ρ^0 photoproduction on lead, $b = 428 \pm 6 \text{ (stat.)} \pm 15 \text{ (syst.)} (\text{GeV}/c)^{-2}$ [39]. The figure inset shows an expanded view of the low p_{T}^2 region, and compares the data with two STARlight calculations, with and without an interference between photon emission from the two nuclei [14, 36], which exhibit different trends only at very low p_{T} . The curve with interference is a slightly better match to the data.

The invariant mass dependent cross section for coherent K⁺K⁻ photoproduction is shown in Fig. 2. The data with $p_{\text{T},\text{KK}}^2 > 0.01 (\text{GeV}/c)^2$ are mostly from incoherent photoproduction, and so are not included in the cross sections. The integrated cross section $d\sigma/dy_{\text{KK}} = 3.37 \pm 0.61 \text{ (stat.)} \pm 0.15 \text{ (syst.)} \text{ mb}$ is measured in the mass range $1.1 < M_{\text{KK}} < 1.4 \text{ GeV}/c^2$ for rapidity $|y_{\text{KK}}| < 0.8$ and $p_{\text{T},\text{KK}}^2 < 0.01 (\text{GeV}/c)^2$.

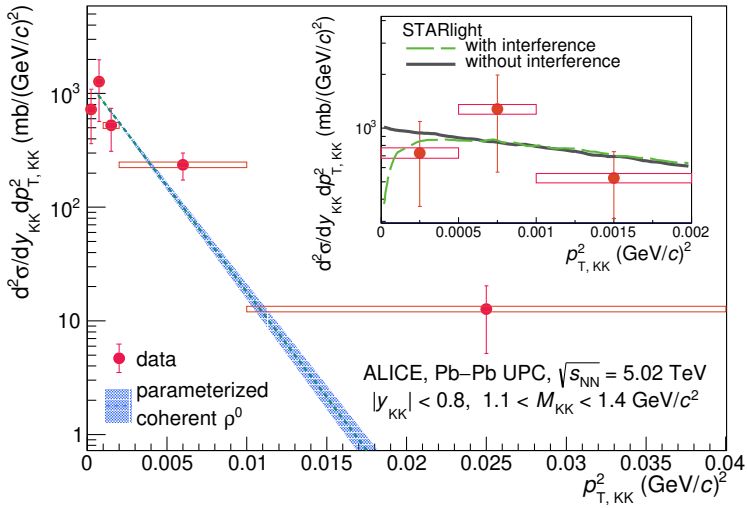


Figure 1: Differential cross section as a function of $p_{T,KK}^2$ for exclusive K^+K^- photoproduction in Pb–Pb UPCs at $\sqrt{s_{NN}} = 5.02$ TeV and $|y_{KK}| < 0.8$. The vertical lines and boxes across the data points represent statistical and systematic uncertainties, respectively. The dashed blue line and band are the result of a fit to an exponential with the fixed slope parameter $b = 428 \pm 6$ (stat.) ± 15 (syst.) $(\text{GeV}/c)^{-2}$, from a previous result on ρ^0 production [39] (see the text for details). The inset shows two curves from STARlight with and without interference between the two photon directions [14, 36].

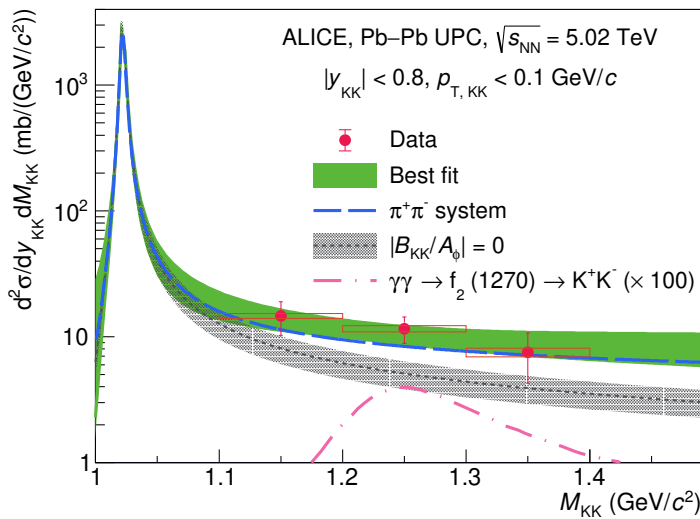


Figure 2: Differential cross section of coherent K^+K^- photoproduction as a function M_{KK} in Pb–Pb UPCs at $\sqrt{s_{NN}} = 5.02$ TeV in $|y_{KK}| < 0.8$. The vertical lines and boxes along the data points represent statistical and systematic uncertainties, respectively. The green solid line presents the best fit result of $|B_{KK}/A_\phi| = 0.28 (\text{GeV}/c^2)^{-1/2}$ and $\varphi = 0.06$ rad together with the 1σ bounds of the fit in a green band. The blue dashed curve shows the best fit with $|B_{\pi\pi}/A_\rho| = 0.54 (\text{GeV}/c^2)^{-1/2}$ [23] and $\varphi = 1.46$ rad (the best-fit values for ρ plus direct $\pi^+\pi^-$) [22]. The black dotted line represents the curves under the hypothesis of $|B_{KK}/A_\phi| = 0$, showing only the $\phi(1020) \rightarrow K^+K^-$ contribution. The gray band indicates the impact of the systematic uncertainty from the $\phi(1020)$ meson cross section, showing a 25% variation.

K⁺K⁻ pairs could be produced by other reactions, such as $\gamma\gamma \rightarrow f_2(1270) \rightarrow K^+K^-$, but calculations indicate that the expected cross section for this process [40] estimated using STARlight [41] is a negligible fraction of the K⁺K⁻ photoproduction cross section as illustrated in Fig. 2.

The measured cross section is fitted to a combination of $\phi(1020) \rightarrow K^+K^-$ and direct K⁺K⁻ production according to Eq. (1). The amplitude of $\phi(1020) \rightarrow K^+K^-$ (A_ϕ) was calculated from previous photoproduction measurements on protons [16, 17, 42] and a Glauber calculation [41], with a branching ratio of $\phi(1020) \rightarrow K^+K^-$ (49.2 \pm 0.5%) [12]. The reference $\phi(1020)$ cross sections did not include a direct K⁺K⁻ contribution. This could have had a small effect on the measured A_ϕ .

A 25% uncertainty in A_ϕ is estimated to account for the uncertainty in the previous measurements [16, 17] and the uncertainty in the Glauber approach [43]. STARlight predictions for ρ^0 production under similar circumstances were 15%–20% below the data [23], while predictions for J/ψ production were about 15%–50% above the data, depending on rapidity [44]. The latter is not surprising, since STARlight does not include gluon shadowing. The $\phi(1020)$ is intermediate in mass, but closer to the ρ^0 , so a $\pm 25\%$ uncertainty in the cross section seems conservative for the $\phi(1020)$.

The black dotted line and surrounding shaded region in Fig. 2 show the ϕ -only prediction, with the 25% uncertainty. The measured cross section is about 2.1σ above the expected $\phi(1020) \rightarrow K^+K^-$ cross section in the range $1.1 < M_{KK} < 1.4 \text{ GeV}/c^2$. Also shown, with a blue dashed line, is the prediction using the values $|B_{\pi\pi}/A_\rho| = 0.54 \pm 0.01 \text{ (stat.)} \pm 0.02 \text{ (syst.) } (\text{GeV}/c^2)^{-1/2}$ [23] and relative phase angle $\varphi = 1.46 \pm 0.11 \text{ (stat.)} \pm 0.07 \text{ (syst.) rad}$ [22] found for ρ^0 plus the direct $\pi^+\pi^-$ system. The resulting $d^2\sigma/dM_{KK}dy_{KK}$ is slightly below, but consistent with, the data points. The best fit of Eq. (1) found the relative fraction of direct K⁺K⁻ contribution with respect to A_ϕ to be $|B_{KK}/A_\phi| = 0.28 \text{ (GeV}/c^2)^{-1/2}$, while the relative phase angle between $\phi(1020) \rightarrow K^+K^-$ and direct K⁺K⁻ is 0.06 rad.

Figure 3 shows the confidence regions for $|B_{KK}/A_\phi|$ and φ . The horseshoe shape of the curves including the first investigation of direct K⁺K⁻ production is because of the large correlations between the two parameters. If the interference is constructive, a small direct K⁺K⁻ component is preferred, while a large K⁺K⁻ component is better fit with destructive interference. The invariant mass-dependent cross section curves corresponding to the 68% confidence region are shown as a 1σ green band in Fig. 3, while the dashed blue band shows the 95% confidence level. We do not include the uncertainty on the cross section $\sigma(\gamma A \rightarrow \phi(1020)A)$ within the figure. As $\sigma(\gamma A \rightarrow \phi(1020)A)$ is reduced or increased, it moves the confidence region left or right, with relatively small changes to the shape. One standard deviation ($\pm 1\sigma$) changes in $\sigma(\gamma A \rightarrow \phi(1020)A)$ move $|B_{KK}/A_\phi|$ by about $\pm 0.15 \text{ (GeV}/c^2)^{-1/2}$ respectively. The best-fit point for the $\pi\pi$ system is fully compatible with the current K⁺K⁻ measurement.

Looking ahead, during LHC Run 3, ALICE will collect a far larger data sample, due to the increased luminosity [45] and continuous-readout data acquisition system [46, 47], which eliminates the need for a restrictive, prescaled trigger. Improved precision measurement of coherent K⁺K⁻ photoproduction by the reduction of statistical uncertainty and an improved tracking will make it possible to further disentangle the resonance and non-resonance contributions with their relative phase angle.

Conclusions. We report the first study of coherent K⁺K⁻ photoproduction in ultra-peripheral collisions at $W_{\gamma Pb,n}$ from 33 to 188 GeV, in the range $1.1 < M_{KK} < 1.4 \text{ GeV}/c^2$ and $|y_{KK}| < 0.8$. The $d^2\sigma/dp_{T,KK}^2 dy_{KK}$ is concentrated below $p_{T,KK}^2 < 0.01 \text{ (GeV}/c)^2$, consistent with coherent photoproduction. The measured $d^2\sigma/dM_{KK}dy_{KK}$ below $p_{T,KK}^2 < 0.01 \text{ (GeV}/c)^2$ is about 2.1σ larger than what is expected from $\phi(1020)$ production alone estimated based on HERA data with a Glauber model calculation, but is consistent with a mixture of $\phi(1020)$ and direct K⁺K⁻ production. The fitted ratio of $\phi(1020)$ production to K⁺K⁻ production is consistent with that seen for the ρ^0 and direct $\pi^+\pi^-$.

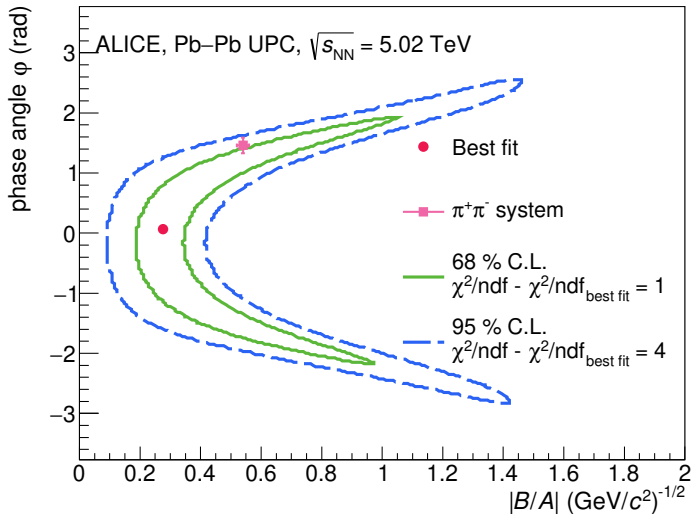


Figure 3: Confidence regions for the relative fraction of direct K⁺K⁻ contribution with respect to the amplitude of $\phi(1020) \rightarrow K^+K^- (|B_{KK}/A_\phi|)$ and the relative phase angle between $\phi(1020) \rightarrow K^+K^-$ and direct K⁺K⁻ (ϕ). The best fit is shown as a red dot at $|B_{KK}/A_\phi| = 0.28 (\text{GeV}/c^2)^{-1/2}$ and $\phi = 0.06 \text{ rad}$ found with $\chi^2/\text{ndf}_{\text{best fit}} = 0.3$, while a pink square at the $|B_{\pi\pi}/A_\rho| = 0.54 \pm 0.01 \text{ (stat.)} \pm 0.02 \text{ (syst.)} (\text{GeV}/c^2)^{-1/2}$ [23] and relative phase angle $\phi = 1.46 \pm 0.11 \text{ (stat.)} \pm 0.07 \text{ (syst.)} \text{ rad}$ [22] indicates the best-fit values for ρ plus direct $\pi^+\pi^-$. The green solid line and blue dashed line represent the boundary of 68% and 95% confidence regions, respectively.

Acknowledgements

The ALICE Collaboration would like to thank all its engineers and technicians for their invaluable contributions to the construction of the experiment and the CERN accelerator teams for the outstanding performance of the LHC complex. The ALICE Collaboration gratefully acknowledges the resources and support provided by all Grid centres and the Worldwide LHC Computing Grid (WLCG) collaboration. The ALICE Collaboration acknowledges the following funding agencies for their support in building and running the ALICE detector: A. I. Alikhanyan National Science Laboratory (Yerevan Physics Institute) Foundation (ANSL), State Committee of Science and World Federation of Scientists (WFS), Armenia; Austrian Academy of Sciences, Austrian Science Fund (FWF): [M 2467-N36] and Nationalstiftung für Forschung, Technologie und Entwicklung, Austria; Ministry of Communications and High Technologies, National Nuclear Research Center, Azerbaijan; Conselho Nacional de Desenvolvimento Científico e Tecnológico (CNPq), Financiadora de Estudos e Projetos (Finep), Fundação de Amparo à Pesquisa do Estado de São Paulo (FAPESP) and Universidade Federal do Rio Grande do Sul (UFRGS), Brazil; Bulgarian Ministry of Education and Science, within the National Roadmap for Research Infrastructures 2020-2027 (object CERN), Bulgaria; Ministry of Education of China (MOEC) , Ministry of Science & Technology of China (MSTC) and National Natural Science Foundation of China (NSFC), China; Ministry of Science and Education and Croatian Science Foundation, Croatia; Centro de Aplicaciones Tecnológicas y Desarrollo Nuclear (CEADEN), Cubaenergía, Cuba; Ministry of Education, Youth and Sports of the Czech Republic, Czech Republic; The Danish Council for Independent Research | Natural Sciences, the VILLUM FONDEN and Danish National Research Foundation (DNRF), Denmark; Helsinki Institute of Physics (HIP), Finland; Commissariat à l'Energie Atomique (CEA) and Institut National de Physique Nucléaire et de Physique des Particules (IN2P3) and Centre National de la Recherche Scientifique (CNRS), France; Bundesministerium für Bildung und Forschung (BMBF) and GSI Helmholtzzentrum für Schwerionenforschung GmbH, Germany; General Secretariat for Research and Technology, Ministry of Education, Research and Religions, Greece; National Research, Development and Innovation Office, Hungary; Department of Atomic Energy Government of India (DAE),

Department of Science and Technology, Government of India (DST), University Grants Commission, Government of India (UGC) and Council of Scientific and Industrial Research (CSIR), India; National Research and Innovation Agency - BRIN, Indonesia; Istituto Nazionale di Fisica Nucleare (INFN), Italy; Japanese Ministry of Education, Culture, Sports, Science and Technology (MEXT) and Japan Society for the Promotion of Science (JSPS) KAKENHI, Japan; Consejo Nacional de Ciencia (CONACYT) y Tecnología, through Fondo de Cooperación Internacional en Ciencia y Tecnología (FONCICYT) and Dirección General de Asuntos del Personal Académico (DGAPA), Mexico; Nederlandse Organisatie voor Wetenschappelijk Onderzoek (NWO), Netherlands; The Research Council of Norway, Norway; Commission on Science and Technology for Sustainable Development in the South (COMSATS), Pakistan; Pontificia Universidad Católica del Perú, Peru; Ministry of Education and Science, National Science Centre and WUT ID-UB, Poland; Korea Institute of Science and Technology Information and National Research Foundation of Korea (NRF), Republic of Korea; Ministry of Education and Scientific Research, Institute of Atomic Physics, Ministry of Research and Innovation and Institute of Atomic Physics and Universitatea Națională de Știință și Tehnologie Politehnica București, Romania; Ministry of Education, Science, Research and Sport of the Slovak Republic, Slovakia; National Research Foundation of South Africa, South Africa; Swedish Research Council (VR) and Knut & Alice Wallenberg Foundation (KAW), Sweden; European Organization for Nuclear Research, Switzerland; Suranaree University of Technology (SUT), National Science and Technology Development Agency (NSTDA) and National Science, Research and Innovation Fund (NSRF via PMU-B B05F650021), Thailand; Turkish Energy, Nuclear and Mineral Research Agency (TENMAK), Turkey; National Academy of Sciences of Ukraine, Ukraine; Science and Technology Facilities Council (STFC), United Kingdom; National Science Foundation of the United States of America (NSF) and United States Department of Energy, Office of Nuclear Physics (DOE NP), United States of America. In addition, individual groups or members have received support from: Czech Science Foundation (grant no. 23-07499S), Czech Republic; European Research Council, Strong 2020 - Horizon 2020 (grant nos. 950692, 824093), European Union; ICSC - Centro Nazionale di Ricerca in High Performance Computing, Big Data and Quantum Computing, European Union - NextGenerationEU; Academy of Finland (Center of Excellence in Quark Matter) (grant nos. 346327, 346328), Finland.

References

- [1] C. A. Bertulani, S. R. Klein, and J. Nystrand, “Physics of ultra-peripheral nuclear collisions”, *Ann. Rev. Nucl. Part. Sci.* **55** (2005) 271–310, arXiv:nucl-ex/0502005.
- [2] A. J. Baltz, “The Physics of Ultraperipheral Collisions at the LHC”, *Phys. Rept.* **458** (2008) 1–171, arXiv:0706.3356 [nucl-ex].
- [3] J. G. Contreras and J. D. Tapia Takaki, “Ultra-peripheral heavy-ion collisions at the LHC”, *Int. J. Mod. Phys. A* **30** (2015) 1542012.
- [4] S. Klein and P. Steinberg, “Photonuclear and Two-photon Interactions at High-Energy Nuclear Colliders”, *Ann. Rev. Nucl. Part. Sci.* **70** (2020) 323–354, arXiv:2005.01872 [nucl-ex].
- [5] S. R. Klein and H. Mäntysaari, “Imaging the nucleus with high-energy photons”, *Nature Rev. Phys.* **1** (2019) 662–674, arXiv:1910.10858 [hep-ex].
- [6] T. H. Bauer, R. D. Spital, D. R. Yennie, and F. M. Pipkin, “The Hadronic Properties of the Photon in High-Energy Interactions”, *Rev. Mod. Phys.* **50** (1978) 261. [Erratum: Rev.Mod.Phys. 51, 407 (1979)].
- [7] **ALEPH** Collaboration, A. Heister *et al.*, “Exclusive production of pion and kaon meson pairs in two photon collisions at LEP”, *Phys. Lett. B* **569** (2003) 140–150.

- [8] **STAR** Collaboration, J. Adam *et al.*, “Measurement of the central exclusive production of charged particle pairs in proton-proton collisions at $\sqrt{s} = 200$ GeV with the STAR detector at RHIC”, *JHEP* **07** (2020) 178, arXiv:2004.11078 [hep-ex].
- [9] P. Söding, “On the Apparent shift of the rho meson mass in photoproduction”, *Phys. Lett.* **19** (1966) 702–704.
- [10] J. D. Jackson, “Remarks on the phenomenological analysis of resonances”, *Nuovo Cim.* **34** (1964) 1644–1666.
- [11] P. Lebiedowicz, O. Nachtmann, and A. Szczurek, “Towards a complete study of central exclusive production of K⁺K⁻ pairs in proton-proton collisions within the tensor Pomeron approach”, *Phys. Rev. D* **98** (2018) 014001, arXiv:1804.04706 [hep-ph].
- [12] **Particle Data Group** Collaboration, R. L. Workman *et al.*, “Review of Particle Physics”, *PTEP* **2022** (2022) 083C01.
- [13] M. G. Ryskin and Y. M. Shabelski, “Elastic rho-prime and phi meson photoproduction and electroproduction with nonresonant background”, *Phys. Atom. Nucl.* **62** (1999) 980–986, arXiv:hep-ph/9712437.
- [14] S. R. Klein and J. Nystrand, “Interference in exclusive vector meson production in heavy ion collisions”, *Phys. Rev. Lett.* **84** (2000) 2330–2333, arXiv:hep-ph/9909237.
- [15] **STAR** Collaboration, B. I. Abelev *et al.*, “Observation of Two-source Interference in the Photoproduction Reaction Au Au → Au Au ρ⁰”, *Phys. Rev. Lett.* **102** (2009) 112301, arXiv:0812.1063 [nucl-ex].
- [16] R. M. Egloff *et al.*, “Measurements of Elastic Rho and Phi Meson Photoproduction Cross-Sections on Protons from 30 GeV to 180 GeV”, *Phys. Rev. Lett.* **43** (1979) 657.
- [17] **ZEUS** Collaboration, M. Derrick *et al.*, “Measurement of elastic φ photoproduction at HERA”, *Phys. Lett. B* **377** (1996) 259–272, arXiv:hep-ex/9601009.
- [18] **ZEUS** Collaboration, S. Chekanov *et al.*, “Exclusive electroproduction of phi mesons at HERA”, *Nucl. Phys. B* **718** (2005) 3–31, arXiv:hep-ex/0504010.
- [19] **H1** Collaboration, F. D. Aaron *et al.*, “Diffractive Electroproduction of rho and phi Mesons at HERA”, *JHEP* **05** (2010) 032, arXiv:0910.5831 [hep-ex].
- [20] **STAR** Collaboration, C. Adler *et al.*, “Coherent ρ⁰ production in ultraperipheral heavy ion collisions”, *Phys. Rev. Lett.* **89** (2002) 272302, arXiv:nucl-ex/0206004.
- [21] **STAR** Collaboration, B. I. Abelev *et al.*, “ρ⁰ photoproduction in ultraperipheral relativistic heavy ion collisions at $\sqrt{s_{NN}} = 200$ GeV”, *Phys. Rev. C* **77** (2008) 034910, arXiv:0712.3320 [nucl-ex].
- [22] **STAR** Collaboration, L. Adamczyk *et al.*, “Coherent diffractive photoproduction of ρ⁰mesons on gold nuclei at 200 GeV/nucleon-pair at the Relativistic Heavy Ion Collider”, *Phys. Rev. C* **96** (2017) 054904, arXiv:1702.07705 [nucl-ex].
- [23] **ALICE** Collaboration, S. Acharya *et al.*, “Coherent photoproduction of ρ⁰ vector mesons in ultra-peripheral Pb-Pb collisions at $\sqrt{s_{NN}} = 5.02$ TeV”, *JHEP* **06** (2020) 035, arXiv:2002.10897 [nucl-ex].

- [24] **ALICE** Collaboration, S. Acharya *et al.*, “First measurement of coherent ρ^0 photoproduction in ultra-peripheral Xe–Xe collisions at sNN=5.44 TeV”, *Phys. Lett. B* **820** (2021) 136481, arXiv:2101.02581 [nucl-ex].
- [25] **CMS** Collaboration, A. M. Sirunyan *et al.*, “Measurement of exclusive $\rho(770)^0$ photoproduction in ultraperipheral pPb collisions at $\sqrt{s_{\text{NN}}} = 5.02$ TeV”, *Eur. Phys. J. C* **79** (2019) 702, arXiv:1902.01339 [hep-ex].
- [26] **H1** Collaboration, V. Andreev *et al.*, “Measurement of Exclusive $\pi^+\pi^-$ and ρ^0 Meson Photoproduction at HERA”, *Eur. Phys. J. C* **80** (2020) 1189, arXiv:2005.14471 [hep-ex].
- [27] **ZEUS** Collaboration, H. Abramowicz *et al.*, “Exclusive electroproduction of two pions at HERA”, *Eur. Phys. J. C* **72** (2012) 1869, arXiv:1111.4905 [hep-ex].
- [28] **STAR** Collaboration, S. R. Klein, “Ultra-Peripheral Collisions with gold ions in STAR”, *PoS DIS2016* (2016) 188, arXiv:1606.02754 [nucl-ex].
- [29] **ALICE** Collaboration, K. Aamodt *et al.*, “The ALICE experiment at the CERN LHC”, *JINST* **3** (2008) S08002.
- [30] **ALICE** Collaboration, B. B. Abelev *et al.*, “Performance of the ALICE Experiment at the CERN LHC”, *Int. J. Mod. Phys. A* **29** (2014) 1430044, arXiv:1402.4476 [nucl-ex].
- [31] **ALICE** Collaboration, E. Abbas *et al.*, “Performance of the ALICE VZERO system”, *JINST* **8** (2013) P10016, arXiv:1306.3130 [nucl-ex].
- [32] **LHC Forward Physics Working Group** Collaboration, K. Akiba *et al.*, “LHC Forward Physics”, *J. Phys. G* **43** (2016) 110201, arXiv:1611.05079 [hep-ph].
- [33] M. Broz *et al.*, “Performance of ALICE AD modules in the CERN PS test beam”, *JINST* **16** (2021) P01017, arXiv:2006.14982 [physics.ins-det].
- [34] **ALICE** Collaboration, K. Aamodt *et al.*, “Alignment of the ALICE Inner Tracking System with cosmic-ray tracks”, *JINST* **5** (2010) P03003, arXiv:1001.0502 [physics.ins-det].
- [35] J. Alme *et al.*, “The ALICE TPC, a large 3-dimensional tracking device with fast readout for ultra-high multiplicity events”, *Nucl. Instrum. Meth. A* **622** (2010) 316–367, arXiv:1001.1950 [physics.ins-det].
- [36] S. R. Klein, J. Nystrand, J. Seger, Y. Gorbunov, and J. Butterworth, “STARlight: A Monte Carlo simulation program for ultra-peripheral collisions of relativistic ions”, *Comput. Phys. Commun.* **212** (2017) 258–268, arXiv:1607.03838 [hep-ph].
- [37] R. Brun, F. Bruyant, F. Carminati, S. Giani, M. Maire, A. McPherson, G. Patrick, and L. Urban, *GEANT: Detector Description and Simulation Tool; Oct 1994*. CERN Program Library. CERN, Geneva, 1993. <https://cds.cern.ch/record/1082634>. Long Writeup W5013.
- [38] **ALICE** Collaboration, S. Acharya *et al.*, “ALICE luminosity determination for Pb–Pb collisions at $\sqrt{s_{\text{NN}}} = 5.02$ TeV”, *JINST* **19** (2024) P02039, arXiv:2204.10148 [nucl-ex].
- [39] **ALICE** Collaboration, J. Adam *et al.*, “Coherent ρ^0 photoproduction in ultra-peripheral Pb–Pb collisions at $\sqrt{s_{\text{NN}}} = 2.76$ TeV”, *JHEP* **09** (2015) 095, arXiv:1503.09177 [nucl-ex].
- [40] A. J. Baltz, Y. Gorbunov, S. R. Klein, and J. Nystrand, “Two-Photon Interactions with Nuclear Breakup in Relativistic Heavy Ion Collisions”, *Phys. Rev. C* **80** (2009) 044902, arXiv:0907.1214 [nucl-ex].

- [41] S. Klein and J. Nystrand, “Exclusive vector meson production in relativistic heavy ion collisions”, *Phys. Rev. C* **60** (1999) 014903, arXiv:hep-ph/9902259.
- [42] J. A. Crittenden, “Exclusive production of neutral vector mesons at the electron - proton collider HERA”, arXiv:hep-ex/9704009.
- [43] L. Frankfurt, V. Guzey, M. Strikman, and M. Zhalov, “Nuclear shadowing in photoproduction of ρ mesons in ultraperipheral nucleus collisions at RHIC and the LHC”, *Phys. Lett. B* **752** (2016) 51–58, arXiv:1506.07150 [hep-ph].
- [44] ALICE Collaboration, S. Acharya *et al.*, “Coherent J/ψ and ψ' photoproduction at midrapidity in ultra-peripheral Pb-Pb collisions at $\sqrt{s_{\text{NN}}} = 5.02$ TeV”, *Eur. Phys. J. C* **81** (2021) 712, arXiv:2101.04577 [nucl-ex].
- [45] Z. Citron *et al.*, “Report from Working Group 5: Future physics opportunities for high-density QCD at the LHC with heavy-ion and proton beams”, *CERN Yellow Rep. Monogr.* **7** (2019) 1159–1410, arXiv:1812.06772 [hep-ph].
- [46] P. Buncic, M. Krzewicki, and P. Vande Vyvre, “Technical Design Report for the Upgrade of the Online-Offline Computing System.” CERN-LHCC-2015-006, 2015.
<https://cds.cern.ch/record/2011297>.
- [47] ALICE Collaboration, “Upgrade of the ALICE Time Projection Chamber.” CERN-LHCC-2013-020, 2013. <https://cds.cern.ch/record/1622286>.

A The ALICE Collaboration

- S. Acharya ¹²⁸, D. Adamová ⁸⁷, G. Aglieri Rinella ³³, M. Agnello ³⁰, N. Agrawal ⁵², Z. Ahammed ¹³⁶, S. Ahmad ¹⁶, S.U. Ahn ⁷², I. Ahuja ³⁸, A. Akindinov ¹⁴², M. Al-Turany ⁹⁸, D. Aleksandrov ¹⁴², B. Alessandro ⁵⁷, H.M. Alfanda ⁶, R. Alfaro Molina ⁶⁸, B. Ali ¹⁶, A. Alici ²⁶, N. Alizadehvandchali ¹¹⁷, A. Alkin ³³, J. Alme ²¹, G. Alocco ⁵³, T. Alt ⁶⁵, A.R. Altamura ⁵¹, I. Altsybeev ⁹⁶, J.R. Alvarado ⁴⁵, M.N. Anaam ⁶, C. Andrei ⁴⁶, N. Andreou ¹¹⁶, A. Andronic ¹²⁷, E. Andronov ¹⁴², V. Anguelov ⁹⁵, F. Antinori ⁵⁵, P. Antonioli ⁵², N. Apadula ⁷⁵, L. Aphectche ¹⁰⁴, H. Appelshäuser ⁶⁵, C. Arata ⁷⁴, S. Arcelli ²⁶, M. Aresti ²³, R. Arnaldi ⁵⁷, J.G.M.C.A. Arneiro ¹¹¹, I.C. Arsene ²⁰, M. Arslanok ¹³⁹, A. Augustinus ³³, R. Averbbeck ⁹⁸, M.D. Azmi ¹⁶, H. Baba ¹²⁵, A. Badalà ⁵⁴, J. Bae ¹⁰⁵, Y.W. Baek ⁴¹, X. Bai ¹²¹, R. Bailhache ⁶⁵, Y. Bailung ⁴⁹, R. Bala ⁹², A. Balbino ³⁰, A. Baldissari ¹³¹, B. Balis ², D. Banerjee ⁴, Z. Banoo ⁹², F. Barile ³², L. Barioglio ⁹⁶, M. Barlou ⁷⁹, B. Barman ⁴², G.G. Barnaföldi ⁴⁷, L.S. Barnby ⁸⁶, E. Barreau ¹⁰⁴, V. Barret ¹²⁸, L. Barreto ¹¹¹, C. Bartels ¹²⁰, K. Barth ³³, E. Bartsch ⁶⁵, N. Bastid ¹²⁸, S. Basu ⁷⁶, G. Batigne ¹⁰⁴, D. Battistini ⁹⁶, B. Batyunya ¹⁴³, D. Baur ⁴⁸, J.L. Bazo Alba ¹⁰², I.G. Bearden ⁸⁴, C. Beattie ¹³⁹, P. Becht ⁹⁸, D. Behera ⁴⁹, I. Belikov ¹³⁰, A.D.C. Bell Hechavarria ¹²⁷, F. Bellini ²⁶, R. Bellwied ¹¹⁷, S. Belokurova ¹⁴², L.G.E. Beltran ¹¹⁰, Y.A.V. Beltran ⁴⁵, G. Bencedi ⁴⁷, S. Beole ²⁵, Y. Berdnikov ¹⁴², A. Berdnikova ⁹⁵, L. Bergmann ⁹⁵, M.G. Besoiu ⁶⁴, L. Betev ³³, P.P. Bhaduri ¹³⁶, A. Bhasin ⁹², M.A. Bhat ⁴, B. Bhattacharjee ⁴², L. Bianchi ²⁵, N. Bianchi ⁵⁰, J. Bielčík ³⁶, J. Bielčíková ⁸⁷, A.P. Bigot ¹³⁰, A. Bilandzic ⁹⁶, G. Biro ⁴⁷, S. Biswas ⁴, N. Bize ¹⁰⁴, J.T. Blair ¹⁰⁹, D. Blau ¹⁴², M.B. Blidaru ⁹⁸, N. Bluhme ³⁹, C. Blume ⁶⁵, G. Boca ^{22,56}, F. Bock ⁸⁸, T. Bodova ²¹, S. Boi ²³, J. Bok ¹⁷, L. Boldizsár ⁴⁷, M. Bombara ³⁸, P.M. Bond ³³, G. Bonomi ^{135,56}, H. Borel ¹³¹, A. Borissov ¹⁴², A.G. Borquez Carcamo ⁹⁵, H. Bossi ¹³⁹, E. Botta ²⁵, Y.E.M. Bouziani ⁶⁵, L. Bratrud ⁶⁵, P. Braun-Munzinger ⁹⁸, M. Bregant ¹¹¹, M. Broz ³⁶, G.E. Bruno ^{97,32}, M.D. Buckland ²⁴, D. Budnikov ¹⁴², H. Buesching ⁶⁵, S. Bufalino ³⁰, P. Buhler ¹⁰³, N. Burmasov ¹⁴², Z. Buthelezi ^{69,124}, A. Bylinkin ²¹, S.A. Bysiak ¹⁰⁸, J.C. Cabanillas Noris ¹¹⁰, M. Cai ⁶, H. Caines ¹³⁹, A. Caliva ²⁹, E. Calvo Villar ¹⁰², J.M.M. Camacho ¹¹⁰, P. Camerini ²⁴, F.D.M. Canedo ¹¹¹, S.L. Cantway ¹³⁹, M. Carabas ¹¹⁴, A.A. Carballo ³³, F. Carnesecchi ³³, R. Caron ¹²⁹, L.A.D. Carvalho ¹¹¹, J. Castillo Castellanos ¹³¹, F. Catalano ^{33,25}, C. Ceballos Sanchez ¹⁴³, I. Chakaberia ⁷⁵, P. Chakraborty ⁴⁸, S. Chandra ¹³⁶, S. Chapelard ³³, M. Chartier ¹²⁰, S. Chattopadhyay ¹³⁶, S. Chattopadhyay ¹⁰⁰, T. Cheng ^{98,6}, C. Cheshkov ¹²⁹, B. Cheynis ¹²⁹, V. Chibante Barroso ³³, D.D. Chinellato ¹¹², E.S. Chizzali ^{II,96}, J. Cho ⁵⁹, S. Cho ⁵⁹, P. Chochula ³³, D. Choudhury ⁴², P. Christakoglou ⁸⁵, C.H. Christensen ⁸⁴, P. Christiansen ⁷⁶, T. Chujo ¹²⁶, M. Ciacco ³⁰, C. Cicalo ⁵³, M.R. Ciupek ⁹⁸, G. Clai^{III,52}, F. Colamaria ⁵¹, J.S. Colburn ¹⁰¹, D. Colella ^{97,32}, M. Colocci ²⁶, M. Concas ³³, G. Conesa Balbastre ⁷⁴, Z. Conesa del Valle ¹³², G. Contin ²⁴, J.G. Contreras ³⁶, M.L. Coquet ¹³¹, P. Cortese ^{134,57}, M.R. Cosentino ¹¹³, F. Costa ³³, S. Costanza ^{22,56}, C. Cot ¹³², J. Crkovská ⁹⁵, P. Crochet ¹²⁸, R. Cruz-Torres ⁷⁵, P. Cui ⁶, A. Dainese ⁵⁵, M.C. Danisch ⁹⁵, A. Danu ⁶⁴, P. Das ⁸¹, P. Das ⁴, S. Das ⁴, A.R. Dash ¹²⁷, S. Dash ⁴⁸, A. De Caro ²⁹, G. de Cataldo ⁵¹, J. de Cuveland ³⁹, A. De Falco ²³, D. De Gruttola ²⁹, N. De Marco ⁵⁷, C. De Martin ²⁴, S. De Pasquale ²⁹, R. Deb ¹³⁵, R. Del Grande ⁹⁶, L. Dello Stritto ^{33,29}, W. Deng ⁶, P. Dhankher ¹⁹, D. Di Bari ³², A. Di Mauro ³³, B. Diab ¹³¹, R.A. Diaz ^{143,7}, T. Dietel ¹¹⁵, Y. Ding ⁶, J. Ditzel ⁶⁵, R. Divià ³³, D.U. Dixit ¹⁹, Ø. Djuvsland ²¹, U. Dmitrieva ¹⁴², A. Dobrin ⁶⁴, B. Dönigus ⁶⁵, J.M. Dubinski ¹³⁷, A. Dubla ⁹⁸, S. Dudi ⁹¹, P. Dupieux ¹²⁸, M. Durkac ¹⁰⁷, N. Dzalaiova ¹³, T.M. Eder ¹²⁷, R.J. Ehlers ⁷⁵, F. Eisenhut ⁶⁵, R. Ejima ⁹³, D. Elia ⁵¹, B. Erasmus ¹⁰⁴, F. Ercolelli ²⁶, B. Espagnon ¹³², G. Eulisse ³³, D. Evans ¹⁰¹, S. Evdokimov ¹⁴², L. Fabbietti ⁹⁶, M. Faggin ²⁸, J. Faivre ⁷⁴, F. Fan ⁶, W. Fan ⁷⁵, A. Fantoni ⁵⁰, M. Fasel ⁸⁸, A. Feliciello ⁵⁷, G. Feofilov ¹⁴², A. Fernández Téllez ⁴⁵, L. Ferrandi ¹¹¹, M.B. Ferrer ³³, A. Ferrero ¹³¹, C. Ferrero ^{IV,57}, A. Ferretti ²⁵, V.J.G. Feuillard ⁹⁵, V. Filova ³⁶, D. Finogeev ¹⁴², F.M. Fionda ⁵³, E. Flatland ³³, F. Flor ¹¹⁷, A.N. Flores ¹⁰⁹, S. Foertsch ⁶⁹, I. Fokin ⁹⁵, S. Fokin ¹⁴², E. Fragiocomo ⁵⁸, E. Frajna ⁴⁷, U. Fuchs ³³, N. Funicello ²⁹, C. Furget ⁷⁴, A. Furs ¹⁴², T. Fusayasu ⁹⁹, J.J. Gaardhøje ⁸⁴, M. Gagliardi ²⁵, A.M. Gago ¹⁰², T. Gahlaut ⁴⁸, C.D. Galvan ¹¹⁰, D.R. Gangadharan ¹¹⁷, P. Ganoti ⁷⁹, C. Garabatos ⁹⁸, T. García Chávez ⁴⁵, E. Garcia-Solis ⁹, C. Gargiulo ³³, P. Gasik ⁹⁸, A. Gautam ¹¹⁹, M.B. Gay Ducati ⁶⁷, M. Germain ¹⁰⁴, A. Ghimouz ¹²⁶, C. Ghosh ¹³⁶, M. Giacalone ⁵², G. Gioachin ³⁰, P. Giubellino ^{98,57}, P. Giubilato ²⁸, A.M.C. Glaenzer ¹³¹, P. Glässel ⁹⁵, E. Glimos ¹²³, D.J.Q. Goh ⁷⁷, V. Gonzalez ¹³⁸, P. Gordeev ¹⁴², M. Gorgon ², K. Goswami ⁴⁹, S. Gotovac ³⁴, V. Grabski ⁶⁸, L.K. Graczykowski ¹³⁷, E. Grecka ⁸⁷, A. Grelli ⁶⁰, C. Grigoras ³³, V. Grigoriev ¹⁴², S. Grigoryan ^{143,1}, F. Grossa ³³, J.F. Grosse-Oetringhaus ³³, R. Grossi ⁹⁸, D. Grund ³⁶, N.A. Grunwald ⁹⁵, G.G. Guardiano ¹¹², R. Guernane ⁷⁴, M. Guilbaud ¹⁰⁴, K. Gulbrandsen ⁸⁴, T. Gündem ⁶⁵, T. Gunji ¹²⁵,

- W. Guo ⁶, A. Gupta ⁹², R. Gupta ⁹², R. Gupta ⁴⁹, K. Gwizdziel ¹³⁷, L. Gyulai ⁴⁷, C. Hadjidakis ¹³², F.U. Haider ⁹², S. Haidlova ³⁶, M. Haldar⁴, H. Hamagaki ⁷⁷, A. Hamdi ⁷⁵, Y. Han ¹⁴⁰, B.G. Hanley ¹³⁸, R. Hannigan ¹⁰⁹, J. Hansen ⁷⁶, J.W. Harris ¹³⁹, A. Harton ⁹, M.V. Hartung ⁶⁵, H. Hassan ¹¹⁸, D. Hatzifotiadou ⁵², P. Hauer ⁴³, L.B. Havener ¹³⁹, E. Hellbär ⁹⁸, H. Helstrup ³⁵, M. Hemmer ⁶⁵, T. Herman ³⁶, G. Herrera Corral ⁸, F. Herrmann ¹²⁷, S. Herrmann ¹²⁹, K.F. Hetland ³⁵, B. Heybeck ⁶⁵, H. Hillemanns ³³, B. Hippolyte ¹³⁰, F.W. Hoffmann ⁷¹, B. Hofman ⁶⁰, G.H. Hong ¹⁴⁰, M. Horst ⁹⁶, A. Horzyk ², Y. Hou ⁶, P. Hristov ³³, C. Hughes ¹²³, P. Huhn ⁶⁵, L.M. Huhta ¹¹⁸, T.J. Humanic ⁸⁹, A. Hutson ¹¹⁷, D. Hutter ³⁹, M.C. Hwang ¹⁹, R. Ilkaev ¹⁴², H. Ilyas ¹⁴, M. Inaba ¹²⁶, G.M. Innocenti ³³, M. Ippolitov ¹⁴², A. Isakov ^{85,87}, T. Isidori ¹¹⁹, M.S. Islam ¹⁰⁰, M. Ivanov ¹³, M. Ivanov ⁹⁸, V. Ivanov ¹⁴², K.E. Iversen ⁷⁶, M. Jablonski ², B. Jacak ^{19,75}, N. Jacazio ²⁶, P.M. Jacobs ⁷⁵, S. Jadlovska ¹⁰⁷, J. Jadlovsky ¹⁰⁷, S. Jaelani ⁸³, C. Jahnke ¹¹¹, M.J. Jakubowska ¹³⁷, M.A. Janik ¹³⁷, T. Janson ⁷¹, S. Ji ¹⁷, S. Jia ¹⁰, A.A.P. Jimenez ⁶⁶, F. Jonas ^{75,88,127}, D.M. Jones ¹²⁰, J.M. Jowett ^{33,98}, J. Jung ⁶⁵, M. Jung ⁶⁵, A. Junique ³³, A. Jusko ¹⁰¹, J. Kaewjai ¹⁰⁶, P. Kalinak ⁶¹, A.S. Kalteyer ⁹⁸, A. Kalweit ³³, A. Karasu Uysal ^{V,73}, D. Karatovic ⁹⁰, O. Karavichev ¹⁴², T. Karavicheva ¹⁴², P. Karczmarczyk ¹³⁷, E. Karpechev ¹⁴², M.J. Karwowska ^{33,137}, U. Kebschull ⁷¹, R. Keidel ¹⁴¹, D.L.D. Keijdener ⁶⁰, M. Keil ³³, B. Ketzer ⁴³, S.S. Khade ⁴⁹, A.M. Khan ¹²¹, S. Khan ¹⁶, A. Khanzadeev ¹⁴², Y. Kharlov ¹⁴², A. Khatun ¹¹⁹, A. Khuntia ³⁶, Z. Khuranova ⁶⁵, B. Kileng ³⁵, B. Kim ¹⁰⁵, C. Kim ¹⁷, D.J. Kim ¹¹⁸, E.J. Kim ⁷⁰, J. Kim ¹⁴⁰, J. Kim ⁵⁹, J. Kim ⁷⁰, M. Kim ¹⁹, S. Kim ¹⁸, T. Kim ¹⁴⁰, K. Kimura ⁹³, S. Kirsch ⁶⁵, I. Kisel ³⁹, S. Kiselev ¹⁴², A. Kisiel ¹³⁷, J.P. Kitowski ², J.L. Klay ⁵, J. Klein ³³, S. Klein ⁷⁵, C. Klein-Bösing ¹²⁷, M. Kleiner ⁶⁵, T. Klemenz ⁹⁶, A. Kluge ³³, C. Kobdaj ¹⁰⁶, T. Kollegger ⁹⁸, A. Kondratyev ¹⁴³, N. Kondratyeva ¹⁴², J. Konig ⁶⁵, S.A. Konigstorfer ⁹⁶, P.J. Konopka ³³, G. Kornakov ¹³⁷, M. Korwieser ⁹⁶, S.D. Koryciak ², A. Kotliarov ⁸⁷, N. Kovacic ⁹⁰, V. Kovalenko ¹⁴², M. Kowalski ¹⁰⁸, V. Kozhuharov ³⁷, I. Králík ⁶¹, A. Kravčáková ³⁸, L. Krcal ^{33,39}, M. Krivda ^{101,61}, F. Krizek ⁸⁷, K. Krizkova Gajdosova ³³, M. Kroesen ⁹⁵, M. Krüger ⁶⁵, D.M. Krupova ³⁶, E. Kryshen ¹⁴², V. Kučera ⁵⁹, C. Kuhn ¹³⁰, P.G. Kuijer ⁸⁵, T. Kumaoka ¹²⁶, D. Kumar ¹³⁶, L. Kumar ⁹¹, N. Kumar ⁹¹, S. Kumar ³², S. Kundu ³³, P. Kurashvili ⁸⁰, A. Kurepin ¹⁴², A.B. Kurepin ¹⁴², A. Kuryakin ¹⁴², S. Kushpil ⁸⁷, V. Kuskov ¹⁴², M. Kutyla ¹³⁷, M.J. Kweon ⁵⁹, Y. Kwon ¹⁴⁰, S.L. La Pointe ³⁹, P. La Rocca ²⁷, A. Lkrathok ¹⁰⁶, M. Lamanna ³³, A.R. Landou ⁷⁴, R. Langoy ¹²², P. Larionov ³³, E. Laudi ³³, L. Lautner ^{33,96}, R. Lavicka ¹⁰³, R. Lea ^{135,56}, H. Lee ¹⁰⁵, I. Legrand ⁴⁶, G. Legras ¹²⁷, J. Lehrbach ³⁹, T.M. Lelek ², R.C. Lemmon ⁸⁶, I. León Monzón ¹¹⁰, M.M. Lesch ⁹⁶, E.D. Lesser ¹⁹, P. Lévai ⁴⁷, X. Li ¹⁰, B.E. Liang-gilman ¹⁹, J. Lien ¹²², R. Lietava ¹⁰¹, I. Likmeta ¹¹⁷, B. Lim ²⁵, S.H. Lim ¹⁷, V. Lindenstruth ³⁹, A. Lindner ⁴⁶, C. Lippmann ⁹⁸, D.H. Liu ⁶, J. Liu ¹²⁰, G.S.S. Liveraro ¹¹², I.M. Lofnes ²¹, C. Loizides ⁸⁸, S. Lokos ¹⁰⁸, J. Lömkér ⁶⁰, P. Loncar ³⁴, X. Lopez ¹²⁸, E. López Torres ⁷, P. Lu ^{98,121}, F.V. Lugo ⁶⁸, J.R. Luhder ¹²⁷, M. Lunardon ²⁸, G. Luparello ⁵⁸, Y.G. Ma ⁴⁰, M. Mager ³³, A. Maire ¹³⁰, E.M. Majerz ², M.V. Makarieva ³⁷, M. Malaev ¹⁴², G. Malfattore ²⁶, N.M. Malik ⁹², Q.W. Malik ²⁰, S.K. Malik ⁹², L. Malinina ^{I,VIII,143}, D. Mallick ^{132,81}, N. Mallick ⁴⁹, G. Mandaglio ^{31,54}, S.K. Mandal ⁸⁰, V. Manko ¹⁴², F. Manso ¹²⁸, V. Manzari ⁵¹, Y. Mao ⁶, R.W. Marcjan ², G.V. Margagliotti ²⁴, A. Margotti ⁵², A. Marín ⁹⁸, C. Markert ¹⁰⁹, P. Martinengo ³³, M.I. Martínez ⁴⁵, G. Martínez García ¹⁰⁴, M.P.P. Martins ¹¹¹, S. Masciocchi ⁹⁸, M. Masera ²⁵, A. Masoni ⁵³, L. Massacrier ¹³², O. Massen ⁶⁰, A. Mastroserio ^{133,51}, O. Matonoha ⁷⁶, S. Mattiuzzo ²⁸, A. Matyja ¹⁰⁸, C. Mayer ¹⁰⁸, A.L. Mazuecos ³³, F. Mazzaschi ²⁵, M. Mazzilli ³³, J.E. Mdhluli ¹²⁴, Y. Melikyan ⁴⁴, A. Menchaca-Rocha ⁶⁸, J.E.M. Mendez ⁶⁶, E. Meninno ¹⁰³, A.S. Menon ¹¹⁷, M. Meres ¹³, Y. Miake ¹²⁶, L. Micheletti ³³, D.L. Mihaylov ⁹⁶, K. Mikhaylov ^{143,142}, D. Miśkowiec ⁹⁸, A. Modak ⁴, B. Mohanty ⁸¹, M. Mohisin Khan ^{VI,16}, M.A. Molander ⁴⁴, S. Monira ¹³⁷, C. Mordasini ¹¹⁸, D.A. Moreira De Godoy ¹²⁷, I. Morozov ¹⁴², A. Morsch ³³, T. Mrnjavac ³³, V. Muccifora ⁵⁰, S. Muhuri ¹³⁶, J.D. Mulligan ⁷⁵, A. Mulliri ²³, M.G. Munhoz ¹¹¹, R.H. Munzer ⁶⁵, H. Murakami ¹²⁵, S. Murray ¹¹⁵, L. Musa ³³, J. Musinsky ⁶¹, J.W. Myrcha ¹³⁷, B. Naik ¹²⁴, A.I. Nambrath ¹⁹, B.K. Nandi ⁴⁸, R. Nania ⁵², E. Nappi ⁵¹, A.F. Nassirpour ¹⁸, A. Nath ⁹⁵, C. Nattrass ¹²³, M.N. Naydenov ³⁷, A. Neagu ²⁰, A. Negru ¹⁴, E. Nekrasova ¹⁴², L. Nellen ⁶⁶, R. Nepeivoda ⁷⁶, S. Nese ²⁰, G. Neskovic ³⁹, N. Nicassio ⁵¹, B.S. Nielsen ⁸⁴, E.G. Nielsen ⁸⁴, S. Nikolaev ¹⁴², S. Nikulin ¹⁴², V. Nikulin ¹⁴², F. Noferini ⁵², S. Noh ¹², P. Nomokonov ¹⁴³, J. Norman ¹²⁰, N. Novitzky ⁸⁸, P. Nowakowski ¹³⁷, A. Nyanin ¹⁴², J. Nystrand ²¹, S. Oh ¹⁸, A. Ohlson ⁷⁶, V.A. Okorokov ¹⁴², J. Oleniacz ¹³⁷, A. Onnerstad ¹¹⁸, C. Oppedisano ⁵⁷, A. Ortiz Velasquez ⁶⁶, J. Otwinowski ¹⁰⁸, M. Oya ⁹³, K. Oyama ⁷⁷, Y. Pachmayer ⁹⁵, S. Padhan ⁴⁸, D. Pagano ^{135,56}, G. Paić ⁶⁶, S. Paisano-Guzmán ⁴⁵, A. Palasciano ⁵¹, S. Panebianco ¹³¹, H. Park ¹²⁶, H. Park ¹⁰⁵, J. Park ⁵⁹, J.E. Parkkila ³³, Y. Patley ⁴⁸,

- B. Paul ²³, H. Pei ⁶, T. Peitzmann ⁶⁰, X. Peng ¹¹, M. Pennisi ²⁵, S. Perciballi ²⁵, D. Peresunko ¹⁴², G.M. Perez ⁷, Y. Pestov ¹⁴², V. Petrov ¹⁴², M. Petrovici ⁴⁶, R.P. Pezzi ^{104,67}, S. Piano ⁵⁸, M. Pikna ¹³, P. Pillot ¹⁰⁴, O. Pinazza ^{52,33}, L. Pinsky ¹¹⁷, C. Pinto ⁹⁶, S. Pisano ⁵⁰, M. Płoskoń ⁷⁵, M. Planinic ⁹⁰, F. Pliquet ⁶⁵, M.G. Poghosyan ⁸⁸, B. Polichtchouk ¹⁴², S. Politano ³⁰, N. Poljak ⁹⁰, A. Pop ⁴⁶, S. Porteboeuf-Houssais ¹²⁸, V. Pozdniakov ^{1,143}, I.Y. Pozos ⁴⁵, K.K. Pradhan ⁴⁹, S.K. Prasad ⁴, S. Prasad ⁴⁹, R. Preghenella ⁵², F. Prino ⁵⁷, C.A. Pruneau ¹³⁸, I. Pshenichnov ¹⁴², M. Puccio ³³, S. Pucillo ²⁵, Z. Pugelova ¹⁰⁷, S. Qiu ⁸⁵, L. Quaglia ²⁵, S. Ragoni ¹⁵, A. Rai ¹³⁹, A. Rakotozafindrabe ¹³¹, L. Ramello ^{134,57}, F. Rami ¹³⁰, T.A. Rancien ⁷⁴, M. Rasa ²⁷, S.S. Räsänen ⁴⁴, R. Rath ⁵², M.P. Rauch ²¹, I. Ravasenga ³³, K.F. Read ^{88,123}, C. Reckziegel ¹¹³, A.R. Redelbach ³⁹, K. Redlich ^{VII,80}, C.A. Reetz ⁹⁸, H.D. Regules-Medel ⁴⁵, A. Rehman ²¹, F. Reidt ³³, H.A. Reme-Ness ³⁵, Z. Rescakova ³⁸, K. Reygers ⁹⁵, A. Riabov ¹⁴², V. Riabov ¹⁴², R. Ricci ²⁹, M. Richter ²⁰, A.A. Riedel ⁹⁶, W. Riegler ³³, A.G. Riffero ²⁵, C. Ristea ⁶⁴, M.V. Rodriguez ³³, M. Rodríguez Cahuantzi ⁴⁵, S.A. Rodríguez Ramírez ⁴⁵, K. Røed ²⁰, R. Rogalev ¹⁴², E. Rogochaya ¹⁴³, T.S. Rogoschinski ⁶⁵, D. Rohr ³³, D. Röhrich ²¹, P.F. Rojas ⁴⁵, S. Rojas Torres ³⁶, P.S. Rokita ¹³⁷, G. Romanenko ²⁶, F. Ronchetti ⁵⁰, A. Rosano ^{31,54}, E.D. Rosas ⁶⁶, K. Roslon ¹³⁷, A. Rossi ⁵⁵, A. Roy ⁴⁹, S. Roy ⁴⁸, N. Rubini ²⁶, D. Ruggiano ¹³⁷, R. Rui ²⁴, P.G. Russek ², R. Russo ⁸⁵, A. Rustamov ⁸², E. Ryabinkin ¹⁴², Y. Ryabov ¹⁴², A. Rybicki ¹⁰⁸, H. Rytkonen ¹¹⁸, J. Ryu ¹⁷, W. Rzesz ¹³⁷, O.A.M. Saarimaki ⁴⁴, S. Sadhu ³², S. Sadovsky ¹⁴², J. Saetre ²¹, K. Šafařík ³⁶, P. Saha ⁴², S.K. Saha ⁴, S. Saha ⁸¹, B. Sahoo ⁴⁸, B. Sahoo ⁴⁹, R. Sahoo ⁴⁹, S. Sahoo ⁶², D. Sahu ⁴⁹, P.K. Sahu ⁶², J. Saini ¹³⁶, K. Sajdakova ³⁸, S. Sakai ¹²⁶, M.P. Salvan ⁹⁸, S. Sambyal ⁹², D. Samitz ¹⁰³, I. Sanna ^{33,96}, T.B. Saramela ¹¹¹, P. Sarma ⁴², V. Sarritzu ²³, V.M. Sarti ⁹⁶, M.H.P. Sas ³³, S. Sawan ⁸¹, E. Scapparone ⁵², J. Schambach ⁸⁸, H.S. Scheid ⁶⁵, C. Schiaua ⁴⁶, R. Schicker ⁹⁵, F. Schlepper ⁹⁵, A. Schmah ⁹⁸, C. Schmidt ⁹⁸, H.R. Schmidt ⁹⁴, M.O. Schmidt ³³, M. Schmidt ⁹⁴, N.V. Schmidt ⁸⁸, A.R. Schmier ¹²³, R. Schotter ¹³⁰, A. Schröter ³⁹, J. Schukraft ³³, K. Schweda ⁹⁸, G. Scioli ²⁶, E. Scomparin ⁵⁷, J.E. Seger ¹⁵, Y. Sekiguchi ¹²⁵, D. Sekihata ¹²⁵, M. Selina ⁸⁵, I. Selyuzhenkov ⁹⁸, S. Senyukov ¹³⁰, J.J. Seo ⁹⁵, D. Serebryakov ¹⁴², L. Serkin ⁶⁶, L. Šerkýně ⁹⁶, A. Sevcenco ⁶⁴, T.J. Shaba ⁶⁹, A. Shabetai ¹⁰⁴, R. Shahoyan ³³, A. Shangaraev ¹⁴², B. Sharma ⁹², D. Sharma ⁴⁸, H. Sharma ⁵⁵, M. Sharma ⁹², S. Sharma ⁷⁷, S. Sharma ⁹², U. Sharma ⁹², A. Shatat ¹³², O. Sheibani ¹¹⁷, K. Shigaki ⁹³, M. Shimomura ⁷⁸, J. Shin ¹², S. Shirinkin ¹⁴², Q. Shou ⁴⁰, Y. Sibirski ¹⁴², S. Siddhanta ⁵³, T. Siemiaczuk ⁸⁰, T.F. Silva ¹¹¹, D. Silvermyr ⁷⁶, T. Simantathammakul ¹⁰⁶, R. Simeonov ³⁷, B. Singh ⁹², B. Singh ⁹⁶, K. Singh ⁴⁹, R. Singh ⁸¹, R. Singh ⁹², R. Singh ⁴⁹, S. Singh ¹⁶, V.K. Singh ¹³⁶, V. Singhal ¹³⁶, T. Sinha ¹⁰⁰, B. Sitar ¹³, M. Sitta ^{134,57}, T.B. Skaali ²⁰, G. Skorodumovs ⁹⁵, M. Slupecki ⁴⁴, N. Smirnov ¹³⁹, R.J.M. Snellings ⁶⁰, E.H. Solheim ²⁰, J. Song ¹⁷, C. Sonnabend ^{33,98}, J.M. Sonneveld ⁸⁵, F. Soramel ²⁸, A.B. Soto-hernandez ⁸⁹, R. Spijkers ⁸⁵, I. Sputowska ¹⁰⁸, J. Staa ⁷⁶, J. Stachel ⁹⁵, I. Stan ⁶⁴, P.J. Steffanic ¹²³, S.F. Stiefelmaier ⁹⁵, D. Stocco ¹⁰⁴, I. Storehaug ²⁰, P. Stratmann ¹²⁷, S. Strazzi ²⁶, A. Sturniolo ^{31,54}, C.P. Stylianidis ⁸⁵, A.A.P. Suaide ¹¹¹, C. Suire ¹³², M. Sukhanov ¹⁴², M. Suljic ³³, R. Sultanov ¹⁴², V. Sumberia ⁹², S. Sumowidagdo ⁸³, S. Swain ⁶², I. Szarka ¹³, M. Szymkowski ¹³⁷, S.F. Taghavi ⁹⁶, G. Taillepied ⁹⁸, J. Takahashi ¹¹², G.J. Tambave ⁸¹, S. Tang ⁶, Z. Tang ¹²¹, J.D. Tapia Takaki ¹¹⁹, N. Tapus ¹¹⁴, L.A. Tarasovicova ¹²⁷, M.G. Tarzila ⁴⁶, G.F. Tassielli ³², A. Tauro ³³, A. Tavira García ¹³², G. Tejeda Muñoz ⁴⁵, A. Telesca ³³, L. Terlizzi ²⁵, C. Terrevoli ¹¹⁷, S. Thakur ⁴, D. Thomas ¹⁰⁹, A. Tikhonov ¹⁴², N. Tiltmann ¹²⁷, A.R. Timmins ¹¹⁷, M. Tkacik ¹⁰⁷, T. Tkacik ¹⁰⁷, A. Toia ⁶⁵, R. Tokumoto ⁹³, K. Tomohiro ⁹³, N. Topilskaya ¹⁴², M. Toppi ⁵⁰, T. Tork ¹³², V.V. Torres ¹⁰⁴, A.G. Torres Ramos ³², A. Trifirò ^{31,54}, A.S. Triolo ^{33,31,54}, S. Tripathy ⁵², T. Tripathy ⁴⁸, S. Trogolo ³³, V. Trubnikov ³, W.H. Trzaska ¹¹⁸, T.P. Trzciński ¹³⁷, A. Tumkin ¹⁴², R. Turrisi ⁵⁵, T.S. Tveter ²⁰, K. Ullaland ²¹, B. Ulukutlu ⁹⁶, A. Uras ¹²⁹, M. Urioni ¹³⁵, G.L. Usai ²³, M. Vala ³⁸, N. Valle ²², L.V.R. van Doremalen ⁶⁰, M. van Leeuwen ⁸⁵, C.A. van Veen ⁹⁵, R.J.G. van Weelden ⁸⁵, P. Vande Vyvre ³³, D. Varga ⁴⁷, Z. Varga ⁴⁷, P. Vargas Torres ⁶⁶, M. Vasileiou ⁷⁹, A. Vasiliev ¹⁴², O. Vázquez Doce ⁵⁰, O. Vazquez Rueda ¹¹⁷, V. Vechernin ¹⁴², E. Vercellin ²⁵, S. Vergara Limón ⁴⁵, R. Verma ⁴⁸, L. Vermunt ⁹⁸, R. Vértesi ⁴⁷, M. Verweij ⁶⁰, L. Vickovic ³⁴, Z. Vilakazi ¹²⁴, O. Villalobos Baillie ¹⁰¹, A. Villani ²⁴, A. Vinogradov ¹⁴², T. Virgili ²⁹, M.M.O. Virta ¹¹⁸, V. Vislavicius ⁷⁶, A. Vodopyanov ¹⁴³, B. Volkel ³³, M.A. Völkl ⁹⁵, S.A. Voloshin ¹³⁸, G. Volpe ³², B. von Haller ³³, I. Vorobyev ³³, N. Vozniuk ¹⁴², J. Vrláková ³⁸, J. Wan ⁴⁰, C. Wang ⁴⁰, D. Wang ⁴⁰, Y. Wang ⁴⁰, Y. Wang ⁶, A. Wegrzynek ³³, F.T. Weiglhofer ³⁹, S.C. Wenzel ³³, J.P. Wessels ¹²⁷, J. Wiechula ⁶⁵, J. Wikne ²⁰, G. Wilk ⁸⁰, J. Wilkinson ⁹⁸, G.A. Willems ¹²⁷, B. Windelband ⁹⁵, M. Winn ¹³¹, J.R. Wright ¹⁰⁹, W. Wu ⁴⁰, Y. Wu ¹²¹, Z. Xiong ¹²¹, R. Xu ⁶, A. Yadav ⁴³, A.K. Yadav ¹³⁶, S. Yalcin ⁷³, Y. Yamaguchi ⁹³, S. Yang ²¹, S. Yano ⁹³, E.R. Yeats ¹⁹, Z. Yin ⁶, I.-K. Yoo ¹⁷, J.H. Yoon ⁵⁹,

H. Yu¹², S. Yuan²¹, A. Yuncu ⁹⁵, V. Zaccolo ²⁴, C. Zampolli ³³, F. Zanone ⁹⁵, N. Zardoshti ³³, A. Zarochentsev ¹⁴², P. Závada ⁶³, N. Zaviyalov¹⁴², M. Zhalov ¹⁴², B. Zhang ⁶, C. Zhang ¹³¹, L. Zhang ⁴⁰, M. Zhang⁶, S. Zhang ⁴⁰, X. Zhang ⁶, Y. Zhang¹²¹, Z. Zhang ⁶, M. Zhao ¹⁰, V. Zherebchevskii ¹⁴², Y. Zhi¹⁰, C. Zhong⁴⁰, D. Zhou ⁶, Y. Zhou ⁸⁴, J. Zhu ^{55,6}, Y. Zhu⁶, S.C. Zugravel ⁵⁷, N. Zurlo ^{135,56}

Affiliation Notes

^I Deceased

^{II} Also at: Max-Planck-Institut fur Physik, Munich, Germany

^{III} Also at: Italian National Agency for New Technologies, Energy and Sustainable Economic Development (ENEA), Bologna, Italy

^{IV} Also at: Dipartimento DET del Politecnico di Torino, Turin, Italy

^V Also at: Yildiz Technical University, Istanbul, Türkiye

^{VI} Also at: Department of Applied Physics, Aligarh Muslim University, Aligarh, India

^{VII} Also at: Institute of Theoretical Physics, University of Wroclaw, Poland

^{VIII} Also at: An institution covered by a cooperation agreement with CERN

Collaboration Institutes

¹ A.I. Alikhanyan National Science Laboratory (Yerevan Physics Institute) Foundation, Yerevan, Armenia

² AGH University of Krakow, Cracow, Poland

³ Bogolyubov Institute for Theoretical Physics, National Academy of Sciences of Ukraine, Kiev, Ukraine

⁴ Bose Institute, Department of Physics and Centre for Astroparticle Physics and Space Science (CAPSS), Kolkata, India

⁵ California Polytechnic State University, San Luis Obispo, California, United States

⁶ Central China Normal University, Wuhan, China

⁷ Centro de Aplicaciones Tecnológicas y Desarrollo Nuclear (CEADEN), Havana, Cuba

⁸ Centro de Investigación y de Estudios Avanzados (CINVESTAV), Mexico City and Mérida, Mexico

⁹ Chicago State University, Chicago, Illinois, United States

¹⁰ China Institute of Atomic Energy, Beijing, China

¹¹ China University of Geosciences, Wuhan, China

¹² Chungbuk National University, Cheongju, Republic of Korea

¹³ Comenius University Bratislava, Faculty of Mathematics, Physics and Informatics, Bratislava, Slovak Republic

¹⁴ COMSATS University Islamabad, Islamabad, Pakistan

¹⁵ Creighton University, Omaha, Nebraska, United States

¹⁶ Department of Physics, Aligarh Muslim University, Aligarh, India

¹⁷ Department of Physics, Pusan National University, Pusan, Republic of Korea

¹⁸ Department of Physics, Sejong University, Seoul, Republic of Korea

¹⁹ Department of Physics, University of California, Berkeley, California, United States

²⁰ Department of Physics, University of Oslo, Oslo, Norway

²¹ Department of Physics and Technology, University of Bergen, Bergen, Norway

²² Dipartimento di Fisica, Università di Pavia, Pavia, Italy

²³ Dipartimento di Fisica dell'Università and Sezione INFN, Cagliari, Italy

²⁴ Dipartimento di Fisica dell'Università and Sezione INFN, Trieste, Italy

²⁵ Dipartimento di Fisica dell'Università and Sezione INFN, Turin, Italy

²⁶ Dipartimento di Fisica e Astronomia dell'Università and Sezione INFN, Bologna, Italy

²⁷ Dipartimento di Fisica e Astronomia dell'Università and Sezione INFN, Catania, Italy

²⁸ Dipartimento di Fisica e Astronomia dell'Università and Sezione INFN, Padova, Italy

²⁹ Dipartimento di Fisica ‘E.R. Caianiello’ dell’Università and Gruppo Collegato INFN, Salerno, Italy

³⁰ Dipartimento DISAT del Politecnico and Sezione INFN, Turin, Italy

³¹ Dipartimento di Scienze MIFT, Università di Messina, Messina, Italy

³² Dipartimento Interateneo di Fisica ‘M. Merlin’ and Sezione INFN, Bari, Italy

³³ European Organization for Nuclear Research (CERN), Geneva, Switzerland

³⁴ Faculty of Electrical Engineering, Mechanical Engineering and Naval Architecture, University of Split, Split, Croatia

- ³⁵ Faculty of Engineering and Science, Western Norway University of Applied Sciences, Bergen, Norway
³⁶ Faculty of Nuclear Sciences and Physical Engineering, Czech Technical University in Prague, Prague, Czech Republic
³⁷ Faculty of Physics, Sofia University, Sofia, Bulgaria
³⁸ Faculty of Science, P.J. Šafárik University, Košice, Slovak Republic
³⁹ Frankfurt Institute for Advanced Studies, Johann Wolfgang Goethe-Universität Frankfurt, Frankfurt, Germany
⁴⁰ Fudan University, Shanghai, China
⁴¹ Gangneung-Wonju National University, Gangneung, Republic of Korea
⁴² Gauhati University, Department of Physics, Guwahati, India
⁴³ Helmholtz-Institut für Strahlen- und Kernphysik, Rheinische Friedrich-Wilhelms-Universität Bonn, Bonn, Germany
⁴⁴ Helsinki Institute of Physics (HIP), Helsinki, Finland
⁴⁵ High Energy Physics Group, Universidad Autónoma de Puebla, Puebla, Mexico
⁴⁶ Horia Hulubei National Institute of Physics and Nuclear Engineering, Bucharest, Romania
⁴⁷ HUN-REN Wigner Research Centre for Physics, Budapest, Hungary
⁴⁸ Indian Institute of Technology Bombay (IIT), Mumbai, India
⁴⁹ Indian Institute of Technology Indore, Indore, India
⁵⁰ INFN, Laboratori Nazionali di Frascati, Frascati, Italy
⁵¹ INFN, Sezione di Bari, Bari, Italy
⁵² INFN, Sezione di Bologna, Bologna, Italy
⁵³ INFN, Sezione di Cagliari, Cagliari, Italy
⁵⁴ INFN, Sezione di Catania, Catania, Italy
⁵⁵ INFN, Sezione di Padova, Padova, Italy
⁵⁶ INFN, Sezione di Pavia, Pavia, Italy
⁵⁷ INFN, Sezione di Torino, Turin, Italy
⁵⁸ INFN, Sezione di Trieste, Trieste, Italy
⁵⁹ Inha University, Incheon, Republic of Korea
⁶⁰ Institute for Gravitational and Subatomic Physics (GRASP), Utrecht University/Nikhef, Utrecht, Netherlands
⁶¹ Institute of Experimental Physics, Slovak Academy of Sciences, Košice, Slovak Republic
⁶² Institute of Physics, Homi Bhabha National Institute, Bhubaneswar, India
⁶³ Institute of Physics of the Czech Academy of Sciences, Prague, Czech Republic
⁶⁴ Institute of Space Science (ISS), Bucharest, Romania
⁶⁵ Institut für Kernphysik, Johann Wolfgang Goethe-Universität Frankfurt, Frankfurt, Germany
⁶⁶ Instituto de Ciencias Nucleares, Universidad Nacional Autónoma de México, Mexico City, Mexico
⁶⁷ Instituto de Física, Universidade Federal do Rio Grande do Sul (UFRGS), Porto Alegre, Brazil
⁶⁸ Instituto de Física, Universidad Nacional Autónoma de México, Mexico City, Mexico
⁶⁹ iThemba LABS, National Research Foundation, Somerset West, South Africa
⁷⁰ Jeonbuk National University, Jeonju, Republic of Korea
⁷¹ Johann-Wolfgang-Goethe Universität Frankfurt Institut für Informatik, Fachbereich Informatik und Mathematik, Frankfurt, Germany
⁷² Korea Institute of Science and Technology Information, Daejeon, Republic of Korea
⁷³ KTO Karatay University, Konya, Turkey
⁷⁴ Laboratoire de Physique Subatomique et de Cosmologie, Université Grenoble-Alpes, CNRS-IN2P3, Grenoble, France
⁷⁵ Lawrence Berkeley National Laboratory, Berkeley, California, United States
⁷⁶ Lund University Department of Physics, Division of Particle Physics, Lund, Sweden
⁷⁷ Nagasaki Institute of Applied Science, Nagasaki, Japan
⁷⁸ Nara Women's University (NWU), Nara, Japan
⁷⁹ National and Kapodistrian University of Athens, School of Science, Department of Physics , Athens, Greece
⁸⁰ National Centre for Nuclear Research, Warsaw, Poland
⁸¹ National Institute of Science Education and Research, Homi Bhabha National Institute, Jatni, India
⁸² National Nuclear Research Center, Baku, Azerbaijan
⁸³ National Research and Innovation Agency - BRIN, Jakarta, Indonesia
⁸⁴ Niels Bohr Institute, University of Copenhagen, Copenhagen, Denmark
⁸⁵ Nikhef, National institute for subatomic physics, Amsterdam, Netherlands
⁸⁶ Nuclear Physics Group, STFC Daresbury Laboratory, Daresbury, United Kingdom

- ⁸⁷ Nuclear Physics Institute of the Czech Academy of Sciences, Husinec-Řež, Czech Republic
⁸⁸ Oak Ridge National Laboratory, Oak Ridge, Tennessee, United States
⁸⁹ Ohio State University, Columbus, Ohio, United States
⁹⁰ Physics department, Faculty of science, University of Zagreb, Zagreb, Croatia
⁹¹ Physics Department, Panjab University, Chandigarh, India
⁹² Physics Department, University of Jammu, Jammu, India
⁹³ Physics Program and International Institute for Sustainability with Knotted Chiral Meta Matter (SKCM2), Hiroshima University, Hiroshima, Japan
⁹⁴ Physikalischs Institut, Eberhard-Karls-Universität Tübingen, Tübingen, Germany
⁹⁵ Physikalischs Institut, Ruprecht-Karls-Universität Heidelberg, Heidelberg, Germany
⁹⁶ Physik Department, Technische Universität München, Munich, Germany
⁹⁷ Politecnico di Bari and Sezione INFN, Bari, Italy
⁹⁸ Research Division and ExtreMe Matter Institute EMMI, GSI Helmholtzzentrum für Schwerionenforschung GmbH, Darmstadt, Germany
⁹⁹ Saga University, Saga, Japan
¹⁰⁰ Saha Institute of Nuclear Physics, Homi Bhabha National Institute, Kolkata, India
¹⁰¹ School of Physics and Astronomy, University of Birmingham, Birmingham, United Kingdom
¹⁰² Sección Física, Departamento de Ciencias, Pontificia Universidad Católica del Perú, Lima, Peru
¹⁰³ Stefan Meyer Institut für Subatomare Physik (SMI), Vienna, Austria
¹⁰⁴ SUBATECH, IMT Atlantique, Nantes Université, CNRS-IN2P3, Nantes, France
¹⁰⁵ Sungkyunkwan University, Suwon City, Republic of Korea
¹⁰⁶ Suranaree University of Technology, Nakhon Ratchasima, Thailand
¹⁰⁷ Technical University of Košice, Košice, Slovak Republic
¹⁰⁸ The Henryk Niewodniczanski Institute of Nuclear Physics, Polish Academy of Sciences, Cracow, Poland
¹⁰⁹ The University of Texas at Austin, Austin, Texas, United States
¹¹⁰ Universidad Autónoma de Sinaloa, Culiacán, Mexico
¹¹¹ Universidade de São Paulo (USP), São Paulo, Brazil
¹¹² Universidade Estadual de Campinas (UNICAMP), Campinas, Brazil
¹¹³ Universidade Federal do ABC, Santo Andre, Brazil
¹¹⁴ Universitatea Nationalala de Stiinta si Tehnologie Politehnica Bucuresti, Bucharest, Romania
¹¹⁵ University of Cape Town, Cape Town, South Africa
¹¹⁶ University of Derby, Derby, United Kingdom
¹¹⁷ University of Houston, Houston, Texas, United States
¹¹⁸ University of Jyväskylä, Jyväskylä, Finland
¹¹⁹ University of Kansas, Lawrence, Kansas, United States
¹²⁰ University of Liverpool, Liverpool, United Kingdom
¹²¹ University of Science and Technology of China, Hefei, China
¹²² University of South-Eastern Norway, Kongsberg, Norway
¹²³ University of Tennessee, Knoxville, Tennessee, United States
¹²⁴ University of the Witwatersrand, Johannesburg, South Africa
¹²⁵ University of Tokyo, Tokyo, Japan
¹²⁶ University of Tsukuba, Tsukuba, Japan
¹²⁷ Universität Münster, Institut für Kernphysik, Münster, Germany
¹²⁸ Université Clermont Auvergne, CNRS/IN2P3, LPC, Clermont-Ferrand, France
¹²⁹ Université de Lyon, CNRS/IN2P3, Institut de Physique des 2 Infinis de Lyon, Lyon, France
¹³⁰ Université de Strasbourg, CNRS, IPHC UMR 7178, F-67000 Strasbourg, France, Strasbourg, France
¹³¹ Université Paris-Saclay, Centre d'Etudes de Saclay (CEA), IRFU, Département de Physique Nucléaire (DPhN), Saclay, France
¹³² Université Paris-Saclay, CNRS/IN2P3, IJCLab, Orsay, France
¹³³ Università degli Studi di Foggia, Foggia, Italy
¹³⁴ Università del Piemonte Orientale, Vercelli, Italy
¹³⁵ Università di Brescia, Brescia, Italy
¹³⁶ Variable Energy Cyclotron Centre, Homi Bhabha National Institute, Kolkata, India
¹³⁷ Warsaw University of Technology, Warsaw, Poland
¹³⁸ Wayne State University, Detroit, Michigan, United States
¹³⁹ Yale University, New Haven, Connecticut, United States

¹⁴⁰ Yonsei University, Seoul, Republic of Korea

¹⁴¹ Zentrum für Technologie und Transfer (ZTT), Worms, Germany

¹⁴² Affiliated with an institute covered by a cooperation agreement with CERN

¹⁴³ Affiliated with an international laboratory covered by a cooperation agreement with CERN.